The Journal of Experimental Biology 205, 3261–3270 (2002)
Printed in Great Britain © The Company of Biologists Limited 2002
JEB4319

Relationship between the membrane potential of the contractile vacuole complex and its osmoregulatory activity in *Paramecium multimicronucleatum*

Heidi K. Grønlien*, Christian Stock†, Marilynn S. Aihara, Richard D. Allen and Yutaka Naitoh‡

Pacific Biomedical Research Center, Snyder Hall 306, University of Hawaii, 2538 The Mall, Honolulu, HI 96822, USA

*Present address: Department of Biology, University of Oslo, PO Box 1051, Blindern, N-0316 Oslo, Norway
†Present address: Physiological Institute, University of Würzburg, Röntgenring 9, D-97070 Würzburg, Germany
‡Author for correspondence (e-mail: naitoh@pbrc.hawaii.edu)

Accepted 18 July 2002

Summary

The electric potential of the contractile vacuole (CV) of *Paramecium multimicronucleatum* was measured *in situ* using microelectrodes, one placed in the CV and the other (reference electrode) in the cytosol of a living cell. The CV potential in a mechanically compressed cell increased in a stepwise manner to a maximal value (approximately 80 mV) early in the fluid-filling phase. This stepwise change was caused by the consecutive reattachment to the CV of the radial arms, where the electrogenic sites are located. The current generated by a single arm was approximately 1.3×10^{-10} A. When cells adapted to a hypotonic solution were exposed to a hypertonic solution, the rate of fluid segregation, R_{CVC}, in the contractile vacuole complex (CVC) diminished at the same time as immunological labelling for V-ATPase disappeared from the radial arms. When the cells were re-exposed to the previous hypotonic solution, the CV potential, which had presumably dropped to near zero after the cell's exposure to the hypertonic solution, gradually returned to its maximum level. This increase in the CV potential occurred in parallel with the recovery of immunological labelling for V-ATPase in the radial arm and the resumption of R_{CVC} or fluid segregation. Concanamycin B, a potent V-ATPase inhibitor, brought about significant decreases in both the CV potential and R_{CVC}. We confirm that (i) the electrogenic site of the radial arm is situated in the decorated spongiome, and (ii) the V-ATPase in the decorated spongiome is electrogenic and is necessary for fluid segregation in the CVC. The CV potential remained at a constant high level (approximately 80 mV), whereas R_{CVC} varied between cells depending on the osmolarity of the adaptation solution. Moreover, the CV potential did not change even though R_{CVC} increased when cells adapted to one osmolarity were exposed to a lower osmolarity, implying that R_{CVC} is not directly correlated with the number of functional V-ATPase complexes present in the CVC.

Key words: contractile vacuole complex, membrane potential, V-ATPase, osmoregulation, fluid segregation activity, exocytotic cycle, *Paramecium multimicronucleatum.*

Introduction

The contractile vacuole complex (CVC) is the osmoregulatory organelle of freshwater ciliates such as *Paramecium* and many other free-living single-celled organisms. The organelle is composed of a central contractile vacuole (CV) surrounded by 5–10 radial arms. Each radial arm consists of an ampulla adjacent to the CV, a collecting canal continuous with the ampulla, a smooth spongiome that branches from the collecting canal and a decorated spongiome that is continuous with the smooth spongiome at its inner end and that ends blindly in the cytosol at its outer periphery. Allen and his colleagues (Allen et al., 1990; Ishida et al., 1993, 1996) reported that a relationship exists between the antibody-labeled decorated spongiome and the fluid segregation activity of the CVC *in vivo*. Also, fluid segregation activity increases concomitant with the recovery of the decorated spongiome after its disruption by hypertonic stimulation of the cell. They also presented immunological evidence to demonstrate the presence of the proton-translocating V-ATPase in the decorated spongiome (Fok et al., 1995).

Recently we described the periodic changes in the electrical potential that exist across the CV membrane. These changes accompany the periodic exocytotic activity of the CV (Tominaga et al., 1998). A CV potential of approximately 80 mV, positive with reference to the cytosol, was seen only when the CV membrane was attached to the radial arms during the CV's fluid-filling phase. We therefore proposed that the CV potential originates from the electrogenic activity of V-ATPases in the membranes of the decorated spongiome that are concentrated along the radial arms.

The primary objective of the present paper was to clarify the relationship between the CV's electrical potential, V-ATPase activity and the rate of fluid segregation in the CVC, R_{CVC}. We examined the CV potential under various external osmotic conditions and in the presence of inhibitors. We found that the CV potential was directly correlated with the number of functional V-ATPase complexes present in the CVC. R_{CVC}, however, was not directly correlated with this number. We propose that the V-ATPase of the decorated spongiome provides energy for the translocation of ions into the CVC lumen, thus setting up and maintaining the osmotic gradient that, according to Stock et al. (2002), allows cytosolic water to enter the CVC lumen by osmosis.

Materials and methods

Cells

Cells of *Paramecium multimicronucleatum* (syngen 2) (Allen and Fok, 1988) were grown in axenic culture medium at 24°C (Fok and Allen, 1979) and were harvested at the late-logarithmic growth phase. The cell density was 4×10^6 to 6×10^6 cells l^{-1}. The cells in the culture medium (12 ml) were centrifuged (approximately 100 ***g***; Centra-CL2 Centrifuge, Needham Heights, MA, USA) for 25 s to form a loose pellet. The cells were then suspended in an appropriate experimental solution. This washing procedure was repeated twice, and the cells were finally suspended in 5 ml of the experimental solution. The cells were kept in this solution for more than 18 h prior to experimentation. All experiments were performed at room temperature (21–24°C).

Experimental solutions

Each experimental solution contained (mmol l^{-1} final concentration) 2.0 KCl, 0.25 $CaCl_2$ and 1.0 Mops–KOH, pH 7.0. The osmolarity of the experimental solution was adjusted by adding different amounts of sorbitol to the solution while its ionic components remained unchanged. Osmolarity was measured using a freezing-point depression osmometer (Micro-Osmometer, Model MO plus, Advanced Instruments, Inc., Norwood, MA, USA). The osmolarity of the solution without sorbitol was approximately 4 mosmol l^{-1}. The osmolarities of the other experimental solutions employed were 24, 64 and 124 mosmol l^{-1}.

Inhibitor-containing solutions were prepared by diluting dimethylsulfoxide (DMSO)-dissolved inhibitors (stock solutions) with the 4 mosmol l^{-1} experimental solution. The inhibitor solutions were (i) 30 nmol l^{-1} (final concentration) concanamycin B, an inhibitor of V-ATPase (Woo et al., 1992) (a gift from Dr K. Miwa, Central Research Laboratories, Ajinomoto Co., Japan; [DMSO]<0.01% v/v), (ii) 40 μmol l^{-1} ethoxyzolamide (EZA), an inhibitor of carbonic anhydrase (Deitmer and Schlue, 1989) (Sigma Chemical Co., St Louis, MO, USA; [DMSO]≤0.1% v/v) and (iii) 1 mmol l^{-1} furosemide, an inhibitor of ion transport in the renal system and in erythrocyte membranes (Brater, 1998; Lauf, 1984) (Sigma Chemical Co., St Louis, MO, USA; [DMSO]≤0.1% v/v). Each inhibitor solution was prepared immediately before experimentation.

Capturing a cell

An adapted cell surrounded by a minute amount of an experimental solution was introduced into a droplet of mineral oil on a coverslip. Some of the experimental solution surrounding the cell was removed through a micropipette to prevent cell movement. The cell was then further arrested by inserting a glass microneedle into it.

Recordings of data

Electrical signals

The tip of a glass capillary microelectrode filled with 3 mol l^{-1} KCl (resistance approximately 70 MΩ) was inserted into the cytosol. A minute amount of the same experimental solution was then reintroduced into the solution surrounding the cell through a micropipette to keep the cell from becoming unduly compressed.

A fine-tipped glass capillary microelectrode filled with 3 mol l^{-1} KCl (resistance approximately 120 MΩ) was inserted into the CV to measure the electrical potential difference between the CV fluid and the cytosol. An approximately 20 ms electrical oscillation of the head amplifier that was connected to the fine-tipped microelectrode was necessary for successful insertion of the electrode into the CV. This electrode also served to inject square-wave electric current pulses (0.2 nA, 100 ms duration) into the CV to determine its input resistance. The input resistance was determined by dividing the potential shift due to injection of a current pulse by the current intensity. A glass microcapillary with a tip diameter of approximately 30 μm was filled with a 2% agar-based experimental solution (resistance approximately 1 MΩ) and placed into the surrounding solution and grounded.

Two electrical signals, one from the electrode inserted into the cytosol (corresponding to the plasma membrane potential) and the other from the electrode inserted into the CV (corresponding to the sum of two potentials, one across the CV membrane and the other across the plasma membrane) were fed into a computer (Power Macintosh 7600/132, Apple Computer Inc. Cupertino, CA, USA) through an A/D–D/A converter (ITC-16; Instrutech Corp., Great Neck, NY, USA). These electrical signals were used to obtain the potential difference between the CV fluid and the cytosol (the CV potential).

Images of the CV

Images of the CV obtained using Nomarski optics (×40 objective on a model DMIRB inverted microscope; Leica Inc. Deerfield, IL, USA) were continuously recorded on VHS videotape using a video cassette recorder (AG 6300, Panasonic Industrial Co., Secaucus, NJ, USA) through a CCD camera (CCD-72, Dage MTI Inc., Michigan City, IN, USA).

Software

Software for feeding the electrical signals into the computer,

for processing the signals and for generating the current pulses required for experimentation was developed on the basis of IgorPro (WaveMetrix, Inc., Lake Oswego, OR, USA) and PulseControl XOP software packages (Herrington et al., 1995). Adobe Photoshop 5 was used to analyse images of the CVC.

Measurement of R_{CVC}

The experimental chamber, with an approximate volume of 20 µl, was first filled with a solution of 0.02% (v/v) poly-L-lysine (Sigma, St Louis, MO, USA). Cells suspended in an experimental solution were introduced into the chamber at one end, while the poly-L-lysine solution was removed from the chamber at the other end by absorption with filter paper. Cells that adhered to the bottom surface of the chamber were subjected to further solution exchange and video-recorded for determining R_{CVC} (Stock et al., 2001).

On the replayed images of the CV, we measured the time between two successive fluid discharges (T) and the maximum diameter of the spherical CV immediately before the start of fluid discharge (D_{max}). R_{CVC} was calculated by dividing the maximum volume of the CV estimated from D_{max} by T and is given in fl s^{-1}

Fluorescent microscopy of the decorated spongiome in the CVC

For examination of the CVC by fluorescence microscopy, formaldehyde-fixed (3% in 50 mmol l^{-1} phosphate buffer, pH 7.4) and cold (–20°C) acetone-permeabilized cells were treated using a monoclonal antibody raised against the decorated spongiome (DS-1) (Allen et al., 1990). This was followed by treatment with fluorescein-isothiocyanate (FITC)-conjugated rabbit anti-mouse IgG. Unbound antibody was washed away using excess buffer solution. The cells were observed using a Zeiss microscope equipped with epifluorescence illumination and a filter appropriate for FITC (B-2E Nikon). Photographs were obtained using Kodak Tri-X film. Values in the text are presented as means ± S.E.M. (N).

Results

Changes in the membrane potential and the input resistance of the CV during exocytotic cycles

Fig. 1A shows a representative trace for the CV membrane potential with reference to the cytosol during four exocytotic cycles (numbered 1–4). The CV potential remained unchanged at a steady level of approximately 79 mV (range 77–80 mV, N=10) during the fluid-filling phase (segments of the trace labeled F). It suddenly decreased to approximately 12 mV (range 11–13 mV, N=10) during the rounding phase (segments of the trace labeled R). It then increased to approximately 26 mV (range 24–27 mV, N=10) when fluid discharge began (segments of the trace labeled D). Immediately after the start of the next fluid-filling phase, it returned to a value slightly higher than that during rounding. The potential then increased steeply to approximately 79 mV and remained at this level during fluid-filling.

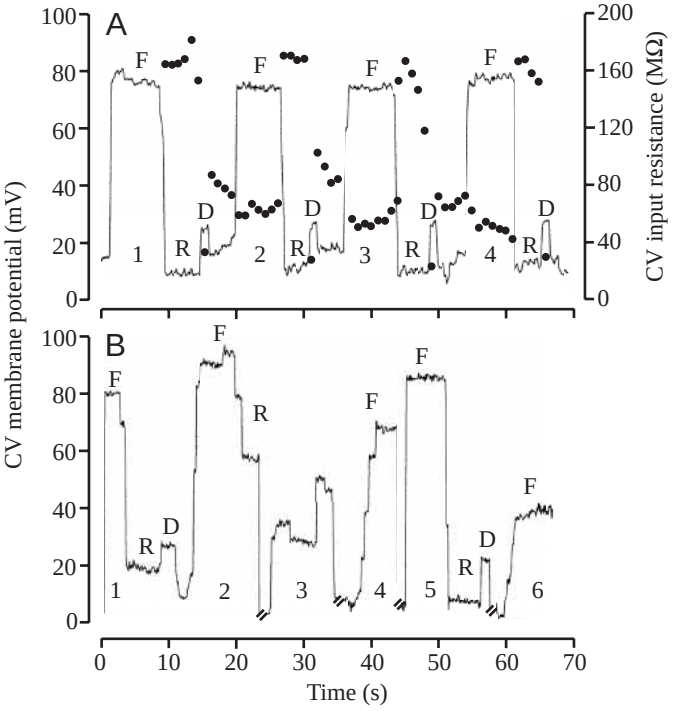

Fig. 1. Representative traces of the electrical potential of the contractile vacuole (CV) fluid with reference to the cytosol in *Paramecium multimicronucleatum* (CV membrane potential) and the input resistance of the CV (A; filled circles). (A) A non-compressed (normal) cell. (B) A mechanically compressed cell. F, R and D above segments of potential traces correspond to the fluid-filling, rounding and fluid-discharging phases of exocytotic cycles of the CV, respectively. Double slashes on the potential trace in B indicate interruptions to the CV membrane potential recording when the electrode tip was no longer in an intact CV during the fluid-discharging phase. See the text for further details. Exocytic cycles are numbered.

The input resistance of the CV (Fig. 1A; filled circles) was approximately 160 MΩ during the rounding phase and decreased to approximately 60 MΩ during the fluid-filling phase. It was approximately 30 MΩ during the fluid-discharging phase.

When a cell was mechanically compressed against the coverslip by removing excess experimental solution and thereby lowering the surface boundary of the mineral oil, the CVC's membrane dynamics during exocytotic cycles were somewhat distorted. Fig. 1B shows a representative trace for the CV membrane potential during six exocytotic cycles (numbered 1–6) in a mechanically compressed cell. In such compressed cells, the electrode tip tended to escape from the CV and to lodge in the cytosol during the fluid-discharging phase. The tip then re-entered the CV as the CV swelled after the start of the fluid-filling phase. Recording of the CV potential was, therefore, interrupted during this phase. Interruptions to the potential recordings are shown by double slashes in Fig. 1B.

The CV potential in a compressed cell increased in a stepwise

manner to a maximum value (usually 80–90 mV) soon after the start of the fluid-filling phase (Fig. 1B; cycles 2 and 4). The CV potential decreased, also in a stepwise manner, after the start of the rounding phase (Fig. 1B; cycles 1, 2 and 5).

Reattachment of the radial arms to the CV in mechanically compressed cells

In mechanically compressed cells, reattachment of the radial arms to the CV after the start of the fluid-filling phase occurred asynchronously. A representative example of asynchronous attachment of the radial arms to the CV during the fluid-filling phase is shown in Fig. 2. In the frame at the upper left labeled 0, which corresponds to the start of a series of 16 frames, the CV was surrounded by four swollen radial arms or ampullae (the proximal ends of the radial arms next to the CV; RA1–RA4). An ampulla is known to swell before it attaches to the CV **(**Hausmann and Allen, 1977**)** and then to narrow after it attaches to the CV. RA1 at 0.6 s, RA2 at 1.0 s, RA3 at 1.8 s and RA4 at 2.6 s (numbers are time in seconds after the start of recording of this series) were narrower than those in the respective previous frames. All radial arms reattached to the CV within 2.8 s. Reattachment of the radial arms in non-compressed cells occurs more-or-less synchronously (data not shown).

Effects of the osmolarity of the adaptation solution on the CV potential, Rcvc and the immunological labeling of the decorated spongiome

As shown in Fig. 3A, the CV potential during the fluid-filling phase (filled squares) was the same in cells that had been adapted to different osmolarities for 18 h: 83.3±2.1 (N=4), 83.9±4.0 (N=8), 87.3±2.0 (N=5) and 83.4±4.9 mV (N=6) in cells adapted to 4, 24, 64 and 124 mosmol l^{-1}, respectively. There were no significant differences between these four values (t-test, P>0.1). By contrast, R_{CVC} differed in cells adapted to different osmolarities: 98.2±50.3 (N=5), 69.9±14.7 (N=10), 19.9±6.2 (P<0.01, N=5) and 20.0±11.8 fl s^{-1} (P<0.01, N=6) in cells adapted to 4, 24, 64 and 124 mosmol l^{-1}, respectively.

Representative fluorescence images of the decorated spongiome of cells adapted to 4, 64 and 124 mosmol l^{-1} are shown in Fig. 3B. No differences in the brightness or appearance of the fluorescence images of the decorated spongiome were observed between cells adapted to different osmolarities.

Recovery of the CV potential, R_{CVC} *and immunological labeling of the decorated spongiome after treatment with a hypertonic solution had ended*

Cells adapted to 4 mosmol l^{-1} for 18 h were exposed to a 124 mosmol l^{-1} solution for 30 min (hypertonic stimulation). The cells were then re-exposed to 4 mosmol l^{-1} adaptation solution. The CV potential during the fluid-filling phase and the R_{CVC} were measured 20, 40, 60, 120 and 240 min after re-exposure to 4 mosmol l^{-1}. Fluorescence images of the decorated spongiome were taken at times corresponding to the times when the CV potential and R_{CVC} were measured. An image of a cell exposed to 124 mosmol l^{-1} for 30 min was taken to show the appearance of its decorated spongiome at time 0 of re-exposure of the cell to 4 mosmol l^{-1}. An image of a cell adapted to 4 mosmol l^{-1} was also taken to serve as a control of the appearance of the decorated spongiome. The CV was

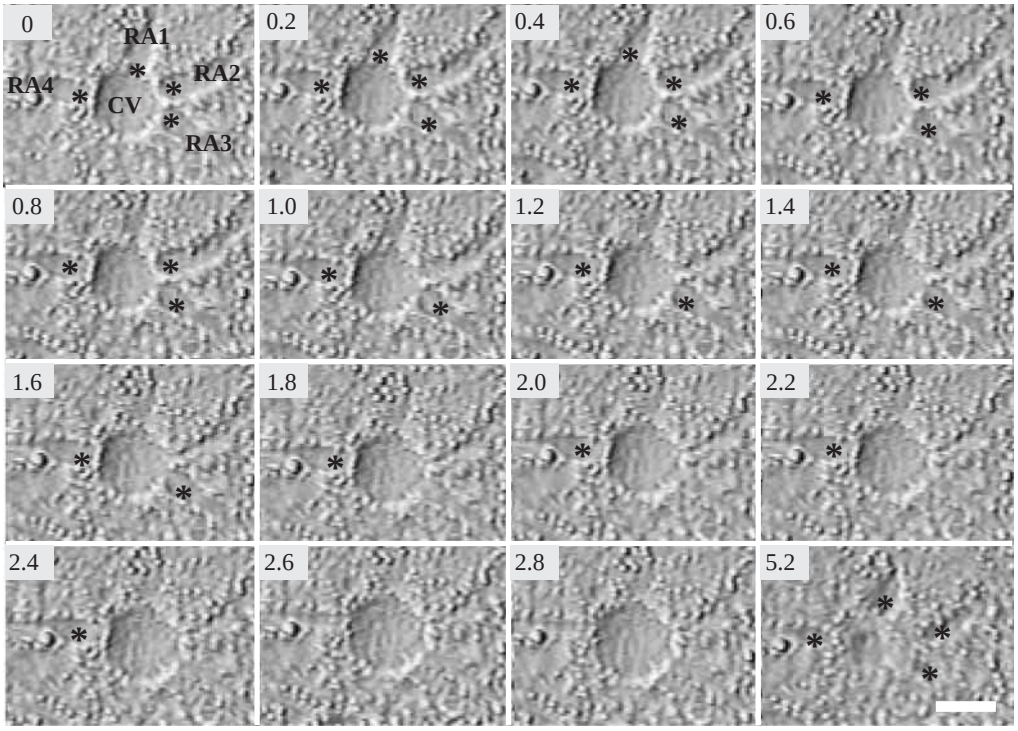

Fig. 2. Consecutive video images of the contractile vacuole in a mechanically compressed cell of *Paramecium multimicronucleatum*. The number at the upper left corner of each frame corresponds to the time (s) when the picture was taken. Time 0 corresponds to the beginning of the series. CV, contractile vacuole; RA, radial arm. Asterisks show swollen portions of the radial arms. The radial arms become thinner after reattachment to the CV. See text for details. Scale bar, 10 μm.

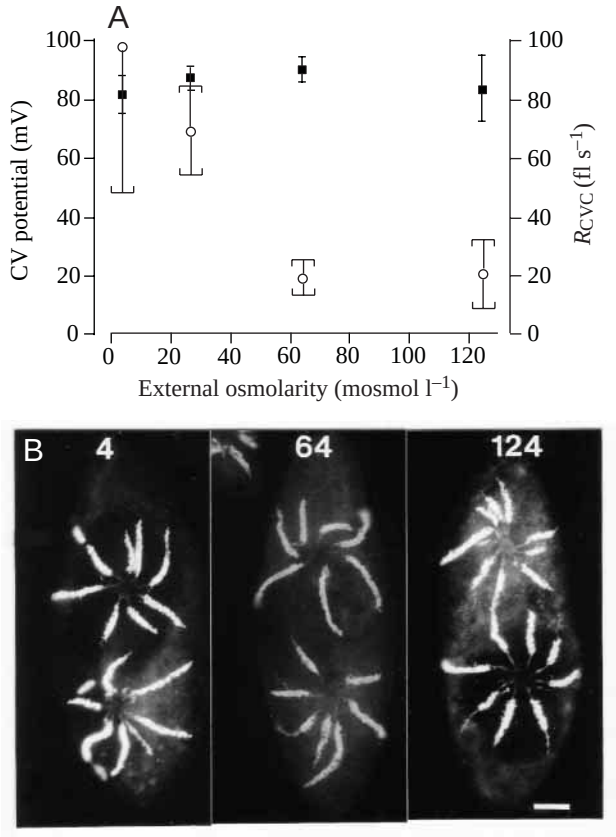

Fig. 3. (A) The contractile vacuole (CV) potential (filled squares) and the rate of fluid segregation in the CV complex (R_{CVC}; open circles) as a function of the osmolarity of adaptation solution in *Paramecium multimicronucleatum*. Values are means ± S.E.M. (N=4–10). (B) DS-1 labelling of the decorated spongiome, visualized by its immunological fluorescence image. The number at the top of each picture corresponds to the osmolarity (mosmol l^{-1}) to which the cell was adapted. Scale bar, 20 μm.

invisible at time 0, the time when the CV potential and R_{CVC} are both assumed to be zero.

As shown in Fig. 4A, the CV potential (filled squares) increased with time after the cells had been re-exposed to 4 mosmol l^{-1}. The potential was 44.0±3.1 (N=5), 50.3±8.4 (N=5), 63.6±2.7 (N=5), 68.8±5.1 (N=6) and 70.6±3.4 mV (N=9) 20, 40, 60, 120 and 240 min after re-exposure to the 4 mosmol l^{-1} solution, respectively. R_{CVC} (open circles) also increased with time after cell re-exposure to 4 mosmol l^{-1} in parallel with the increase in the CV potential. R_{CVC} was 57.7±7.5 (N=5), 80.5±7.1 (N=5), 114.7±8.8 (N=6), 97.0±11.5 (N=7) and 95.3±36.8 fl s^{-1} (N=7) 20, 40, 60, 120 and 240 min after re-exposure to 4 mosmol l^{-1}, respectively.

A representative series of fluorescence images of the decorated spongiome is shown in Fig. 4B. The decorated spongiome, or at least the V-ATPases (Fok et al., 1995), was disrupted and the DS-1 labeling was dispersed into the cytosol during hypertonic stimulation of cells (image labeled 0). A labeled decorated spongiome began to reappear along portions of the radial arms proximal to the CV 20 min after the cells had been re-exposed to 4 mosmol l^{-1} (image labeled 20). The decorated spongiome extended along the radial arms over time, and its fluorescence image after 120 min of re-exposure to 4 mosmol l^{-1} was very similar to that in cells adapted to 4 mosmol l^{-1} for 18 h (compare image labeled 120 with that labeled control).

Table 1. *Effects of hypotonic stimulation on the contractile vacuole potential and rate of fluid segregation in the contractile vacuole*

	Osmolarity of experimental solution (mosmol l^{-1})	
	124	4
CV potential (mV)	80.4±3.4	82.2±3.4
R_{CVC} (fl s^{-1})	20.0±11.8	103.4±18.8

Values are means ± S.E.M. (N=6).
R_{CVC}, rate of fluid segregation in the contractile vacuole (CV).

Effects of hypotonic stimulation on the CV potential and R_{CVC}

Cells adapted to an osmolarity of 124 mosmol l^{-1} for 18 h were exposed to a 4 mosmol l^{-1} solution for 30 min (hypotonic stimulation). The CV potential during the fluid-filling phase and R_{CVC} were then measured. As shown in Table 1, no significant (P>0.1) change in the CV potential occurred in response to exposure of cells adapted to 124 mosmol l^{-1} to 4 mosmol l^{-1}. By contrast, R_{CVC} was significantly (P<0.05) increased from approximately 20 to 103 fl s^{-1} by hypotonic stimulation.

Effects of inhibitors on the CV potential and R_{CVC}

Cells adapted to 4 mosmol l^{-1} were exposed to inhibitors in 4 mosmol l^{-1} solution for 10–30 min. The CV potential during the fluid-filling phase and R_{CVC} were then measured. The inhibitors employed were 30 nmol l^{-1} concanamycin B, 1.0 mmol l^{-1} furosemide and 40 μmol l^{-1} EZA.

As shown in Table 2, exposure of cells to concanamycin B for 30 min brought about a decrease in the CV potential from approximately 82 to 40 mV (a 51% decrease; P<0.05). By contrast, R_{CVC} decreased from approximately 108 to 62 fl s^{-1} (a 43% decrease; P<0.05). The CV potential decreased from approximately 82 to 52 mV (a 37% decrease; P<0.05) after a 10 min exposure to furosemide, while R_{CVC} decreased from approximately 108 to 62 fl s^{-1} (a 43% decrease; P<0.05). Exposure of cells to EZA for 10 min caused a decrease in the CV potential from approximately 82 to 58 mV (a 27% decrease; P<0.05), while R_{CVC} decreased from 108 to 62 fl s^{-1} (a 43% decrease; P<0.05). Exposure of cells to 4 mosmol l^{-1} solution containing 0.1% DMSO, the concentration of this solvent required to dissolve the inhibitors, had no effect on either the CV potential or R_{CVC} (compare the control values for the CV potential and for R_{CVC} in Table 2 with values obtained in the absence of DMSO shown in Fig. 3).

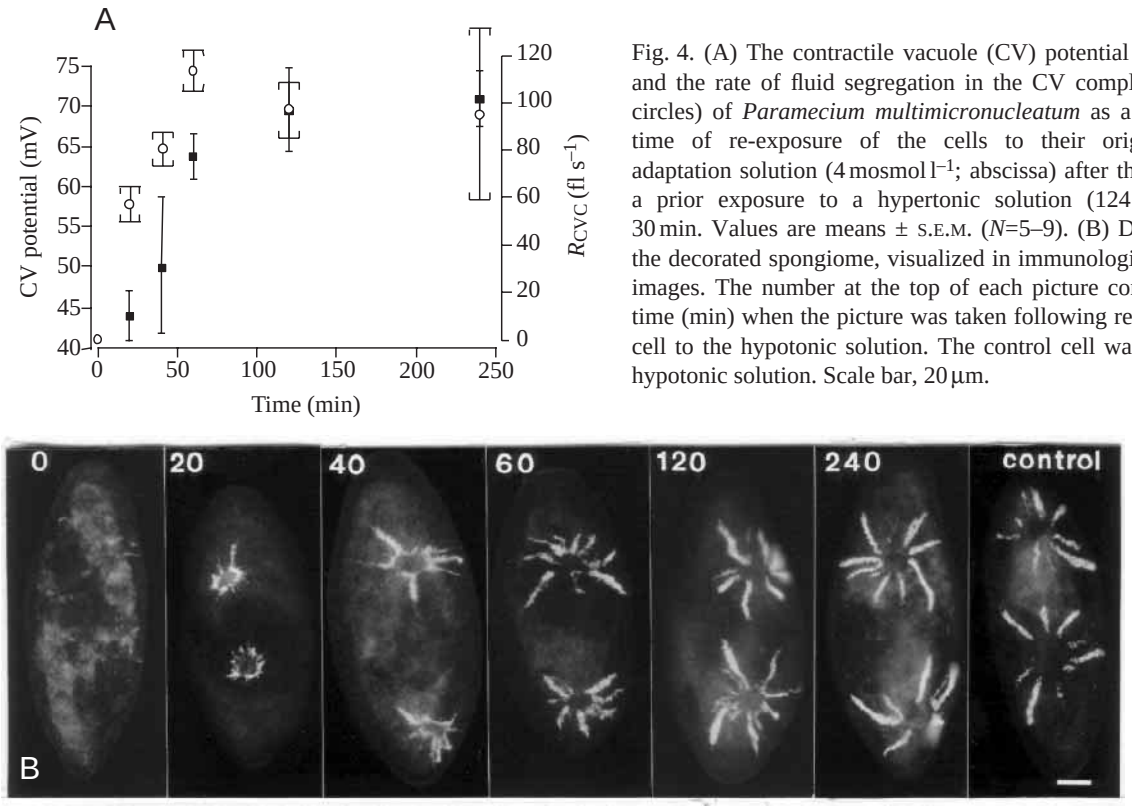

Fig. 4. (A) The contractile vacuole (CV) potential (filled squares), and the rate of fluid segregation in the CV complex (R_{CVC}; open circles) of *Paramecium multimicronucleatum* as a function of the time of re-exposure of the cells to their original hypotonic adaptation solution (4 mosmol l^{-1}; abscissa) after they had received a prior exposure to a hypertonic solution (124 mosmol l^{-1}) for 30 min. Values are means ± S.E.M. (N=5–9). (B) DS-1 labelling of the decorated spongiome, visualized in immunological fluorescence images. The number at the top of each picture corresponds to the time (min) when the picture was taken following re-exposure of the cell to the hypotonic solution. The control cell was adapted to the hypotonic solution. Scale bar, 20 μm.

Discussion

The stepwise changes in the CV potential in a mechanically compressed cell are caused by asynchronous detachment and reattachment of the radial arms to the CV

As shown in Fig. 2, when a cell was mechanically compressed, reattachment of the radial arms to the CV during the early fluid-filling phase did not occur synchronously; instead it occurred more-or-less one at a time. In contrast, reattachment of the radial arms in non-compressed normal cells occurred more-or-less synchronously (data not shown). Mechanical compression of a cell is assumed to disturb the membrane dynamics of the CVC.

As shown in Fig. 1B, the CV potential increased in a stepwise manner to its highest value (70–90 mV) during the early fluid-filling phase in a mechanically compressed cell (see exocytotic cycles 2 and 4). In contrast, as shown in Fig. 1A, in a non-compressed cell, the CV potential generally reached its maximum value of approximately 80 mV without showing discrete stepwise changes during the early fluid-filling phase (see exocytotic cycles 1, 2 and 4; there was a single step in cycle 3).

In a compressed cell, the CV potential decreased in a stepwise manner to its minimum value (10–20 mV) during the early rounding phase (Fig. 1B; exocytotic cycles 1, 2 and 5). In contrast, as shown in Fig. 1A, in a non-compressed cell, the CV potential reached its minimum value (approximately 10 mV) without stepwise changes during the early rounding phase. Detachment of the radial arms from the CV during the early rounding phase also occurred asynchronously in such compressed cells (video data not shown). We conclude that stepwise changes in the CV potential, as seen in mechanically compressed cells, corresponds to the attachment or detachment of individual radial arms from the CV.

These findings support our previous hypothesis that the CV potential observed during the fluid-filling phase is dependent on the electrogenic activity of the radial arms (Tominaga et al., 1998). An equivalent electrical circuit explaining these stepwise changes in the CV potential is presented in Fig. 5B and is discussed below.

Correlating the CV potential during the fluid-filling phase with the presence of the V-ATPase-bearing decorated spongiome in the radial arms and with R_{CVC}

As shown in Fig. 4A, we have demonstrated that the CV potential (filled squares) gradually increases in parallel with an increase in R_{CVC} (open circles) in cells re-exposed to a hypotonic (4 mosmol l^{-1}) adaptation solution after an exposure of 30 min to a hypertonic (124 mosmol l^{-1}) solution. This increase in the CV potential to the control value of approximately 80 mV was accompanied by the reappearance of a monoclonal antibody (DS-1)-immunolabeled decorated spongiome, as illustrated in Fig. 4B. DS-1 labels the V-ATPase on the decorated spongiome (Allen et al., 1990; Fok et al., 1995). These findings support the idea that the CV potential in the fluid-filling phase is generated in the decorated spongiome membrane, where the V-ATPase complexes are situated (Tominaga et al., 1998).

Utilizing DS-1, Ishida et al. (1993) demonstrated that an

Table 2. *Effects of inhibitors on the contractile vacuole potential and the rate of fluid segregation in the contractile vacuole*

		Inhibitor		
	Control	Concanamycin B (30 nmol l^{-1})	Furosemide (1.0 mmol l^{-1})	EZA (40 μmol l^{-1})
CV potential (mV)	81.6±4.4 (5)	40.3±10.7 (6)	52.4±10.5 (10)	58.3±8.8 (10)
R_{CVC} (fl s^{-1})	107.5±13.9 (5)	61.9±18.6 (8)	62.4±16.0 (5)	62.1±6.9 (5)

Values are means ± S.E.M. (*N*).
R_{CVC}, rate of fluid segregation in the contractile vacuole (CV); EZA, ethoxyzolamide.
The control solution had an osmolarity of 4 mosmol l^{-1} and contained 0.1% dimethyl sulfoxide.
Inhibitors were added to 4 mosmol l^{-1} solution.

important site in the fluid segregation activity of the CVC is situated in the decorated spongiome. Ishida et al. (1996) then found that hypertonic stimulation of *Paramecium* cells led to the separation of the V-ATPase-bearing decorated spongiome from the CVC. The R_{CVC} dropped to near zero at the time that the fluorescence of the decorated spongiome was disrupted. Re-exposure of cells to the previous hypotonic solution resulted in the reappearance of the immunologically labeled decorated spongiome around the radial arms as well as to the resumption of the control rate of fluid segregation.

According to Stock et al. (2001), the osmolarity of the cytosol increases rather slowly (taking over 12 h) after cells have been exposed to a hypertonic solution. It is therefore assumed that the cytosolic osmolarity of cells adapted to 4 mosmol l^{-1} does not change significantly during a 30 min exposure to a hypertonic (124 mosmol l^{-1}) solution. It is also assumed that the water permeability of the plasma membrane does not change significantly during this brief exposure to a hypertonic solution (Stock et al., 2001). The rate of osmotic water influx across the plasma membrane after reexposure to a 4 mosmol l^{-1} solution is, therefore, assumed to be similar to that before the 30 min exposure to 124 mosmol l^{-1}. The R_{CVC} must equal the rate of osmotic water influx prior to the cells' exposure to hypertonic solution, i.e. at a time when the decorated spongiome is still intact, or the cell would swell or shrink. The lower R_{CVC} during the early phase of exposure to hypertonic solution, compared with the later stages, can be attributed to the decreased number of functionally active V-ATPase complexes associated with the CVC. This decrease can be attributed to the disruption of the decorated spongiome by hypertonic stimulation. As the number of functional V-ATPase complexes increases over time (as shown by the gradual thickening and lengthening of fluorescence images of the decorated spongiome; Fig. 4B), the fluid segregation also increases, but presumably only to a rate determined by the rate of water entry across the plasma membrane. Thus, the numbers of V-ATPase complexes present on the decorated spongiome and R_{CVC} are not necessarily proportional.

Based on these findings, we conclude that the electrical potential across the spongiome membrane is proportional to the number of functional V-ATPase complexes present in the decorated spongiome. Our finding that concanamycin B, a potent inhibitor of V-ATPase activity (Woo et al., 1992), caused a significant decrease in both the maximum CV potential during the fluid-filling phase and R_{CVC} (Table 2) implies that electrogenic V-ATPase activity is involved in the fluid expulsion activity of the decorated spongiome. The stoichiometric relationship between the CV potential and the number of functional ATPase complexes present should be examined further.

Based on the K^+ and Cl^- activities in the CVs *in vivo*, Stock et al. (2002) proposed that K^+ and Cl^- must be transported in significant amounts across the CVC membrane for water to be transported osmotically from the cytosol to the CVC lumen. These ions would be needed to maintain R_{CVC} at an appropriate level. To understand the mechanism that promotes water transport across the CVC membrane, it is important to know how the V-ATPase-mediated electrical potential across the spongiome membrane is associated with this membrane's hypothetical K^+ and Cl^- transport activity or of other ion transport activities.

The CV potential during the fluid-filling phase remains at the same maximum level in cells adapted to different osmolarities even though their R_{CVC} *varies*

As is clearly shown in Fig. 3A, the CV potential during the fluid-filling phase (filled squares) was maximal and approximately the same (80–90 mV) for cells that had been adapted to different osmolarities (4, 24, 64 and 124 mosmol l^{-1}). By contrast, R_{CVC} changed significantly (P<0.01) as the adaptation osmolarity changed, i.e. it was approximately 98, 70, 20 and 20 fl s^{-1} for cells adapted to 4, 24, 64 and 124 mosmol l^{-1}, respectively. The decorated spongiome appeared to be normal and unaltered in all cells, even when adapted to different osmolarities (Fig. 3B). Moreover, the CV potential during the fluid-filling phase remained unchanged at its maximum level of approximately 80 mV, even though R_{CVC} increased from approximately 20 to 103 fl s^{-1} when cells adapted to 124 mosmol l^{-1} were exposed to a 4 mosmol l^{-1} solution (hypotonic stimulation, Table 1).

These findings imply that (i) the number of functional V-ATPase complexes in the decorated spongiome is nearly constant and at its maximum level in all cells adapted to different osmolarities and (ii) the number of complexes is

unaffected by hypotonic stimulation even though R_{CVC} increases dramatically. Maximal V-ATPase activity might somehow energize the hypothetical K^+ and Cl^- transport system in the CVC membrane (Stock et al., 2002), which can provide the osmotic gradient across the CVC membrane and thereby promote osmotic flow of excess cytosolic water into the CVC lumen.

Furosemide and EZA reduce both the CV potential and R_{CVC}

Furosemide is known to inhibit ion transport in the loop of Henle (Brater, 1998) and erythrocytes (Lauf, 1984; Canessa et al., 1986; Garay et al., 1988). Stock et al. (2002) found that furosemide inhibited transport of K^+ and Cl^- across the plasma membrane of *Paramecium* and caused a decrease in R_{CVC}. We show here that an external application of furosemide (1.0 mmol l^{-1}) reduces the CV potential to approximately 63% of its maximum control value (82 mV; Table 2). R_{CVC} is reduced to approximately 57% of its control value (108 fl s^{-1}; Table 2). Stock et al. (2002) reported that furosemide decreased cytosolic K^+ and Cl^- activities and suggested that these decreases were partially responsible for the decrease in R_{CVC}. It is also possible that furosemide directly inhibits V-ATPase. The effect of cytosolic K^+ activity on V-ATPase activity will need to be examined.

External application of EZA, which is known to inhibit carbonic anhydrase (Deitmer and Schlue, 1989), reduced the CV potential to approximately 71% of its control value (82 mV; Table 2) and R_{CVC} to approximately 57% of its control value (108 fl s^{-1}; Table 2). It is possible that carbonic anhydrase is involved in supplying H^+ for proton translocation by the V-ATPase of the decorated spongiome. In this case, a reduced supply of protons to the V-ATPases could account for the decrease in the CV potential.

The results of these inhibitor experiments also strongly support our suggestion that the V-ATPase-mediated electric potential of the CVC membrane is closely involved in establishing the osmotic gradient across the CVC membrane that is essential for osmotic flow of excess cytosolic water into the CVC lumen.

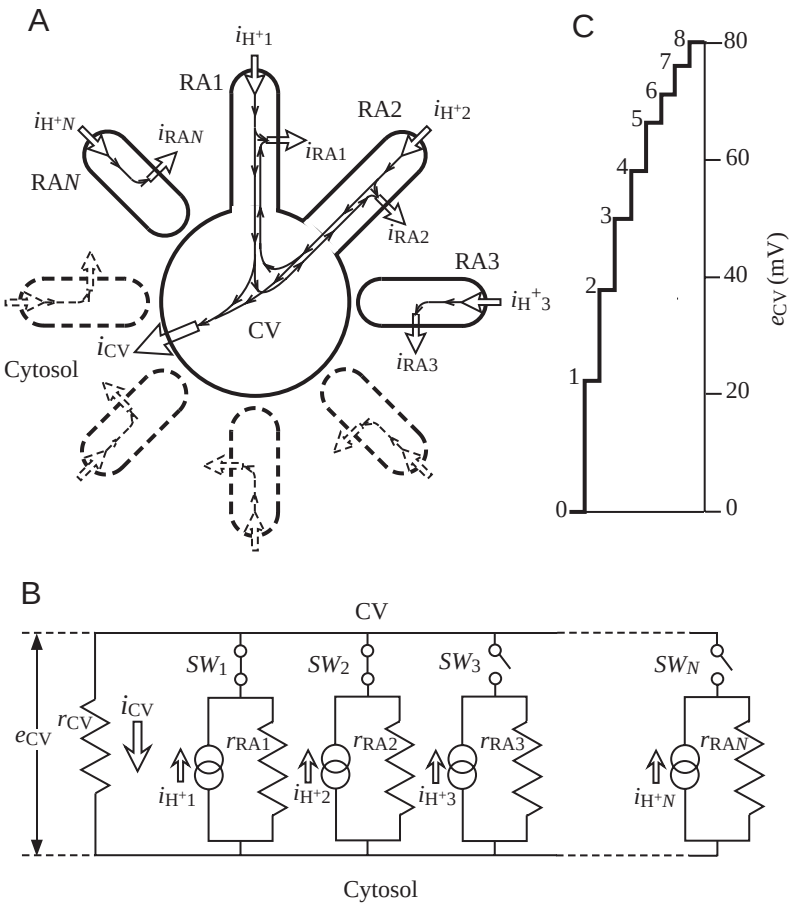

Fig. 5. (A) A schematic representation of the contractile vacuole (CV) complex in *Paramecium multimicronucleatum* to show the pathways of the electric currents generated by V-ATPases in the radial arms. CV, contractile vacuole; RA1–RA*N*, the radial arms 1–*N*, where *N* is the total number of radial arms; i_{H^+}, the current generated in a single radial arm; i_{RA}, the passive current across the radial arm membrane caused by i_{H^+}; i_{CV}, the passive current across the CV membrane caused by i_{H^+} of those radial arms attached to the CV. (B) An electric circuit equivalent to A. r_{CV}, the input resistance of the CV; r_{RA}, the input resistance of a radial arm; SW, a switch corresponding to the attachment of the radial arm to (on) or detachment of the RA from (off) the CV; e_{CV}, CV potential. (C) Simulated stepwise changes in the e_{CV} based on the equivalent circuit (B) as a total of eight radial arms attach to the CV one by one. Numbers to the left signify potential steps as the radial arms are attached to the CV one by one.

Electrical equivalent circuit for the CVC, simulation of the stepwise changes in CV potential as the radial arms attach to the CV and estimation of electric current generated by the V-ATPase activity in a single radial arm

V-ATPase activity can be regarded as a source of constant electric current. A schematic representation of the CVC showing the electric currents due to V-ATPase activity is shown in Fig. 5A, and its corresponding equivalent electrical circuit is shown in Fig. 5B. Each radial arm (RA) generates a constant electric current, i_{H^+}, which produces an electrical potential difference across the radial arm membrane, e_{RA}, that can be written as:

$$e_{RA} = i_{H^+} r_{RA}\,, \qquad (1)$$

where r_{RA} is the electrical resistance corresponding to the input resistance of a single radial arm (see Fig. 5A; RA3, RA*N*). When a radial arm attaches to the CV, i_{H^+} now flows through both r_{RA} and r_{CV}, where r_{CV} is the input resistance of the CV (see Fig. 5A, RA1, RA2). Attachment of the radial arm to the CV corresponds to turning on the switch in the equivalent circuit (SW, Fig. 5B). If we assume that i_{H^+} and r_{RA} are the same for each radial arm in a single CVC, the electric current

through r_{CV} when the radial arms attach to the CV, $i_{CV(N)}$, can be written as:

$$i_{CV(N)} = Ni_{H^+} \frac{r_{RA}}{Nr_{CV} + r_{RA}} , \quad (2)$$

where N is the number of the radial arms attached to the CV. The CV potential, $e_{CV(N)}$, can be written as:

$$e_{CV(N)} = Ni_{H^+} \frac{r_{CV}r_{RA}}{Nr_{CV} + r_{RA}} . \quad (3)$$

Equation 3 is consistent with the stepwise change in the CV potential as the radial arms attach to the CV. The simulated stepwise changes in the CV potential calculated using this equation (Fig. 5C) strikingly resemble the actual stepwise changes in the CV potential shown in Fig. 1B. In this simulation, eight arms attach to the CV one after another. In a mechanically compressed CVC, it is assumed that attachment of the radial arms does not occur strictly one by one, but that some arms attach to the CV simultaneously, so that the number and magnitude of each potential step will vary.

The input resistance of approximately 60 MΩ of the CV during the fluid-filling phase (Fig. 1A) corresponds to the electrical resistance for the overall membrane of the CVC, r_{CVC}. The input resistance of approximately 160 MΩ of the CV during the rounding phase (Fig. 1A) corresponds to the input resistance of the CV only, r_{CV}. r_{RA} can be written as:

$$r_{RA} = \frac{Nr_{CV}r_{CV}}{r_{CV} - r_{CVC}} , \quad (4)$$

where N is the number of radial arms (mean value of N=10; Allen and Naitoh, 2002). By introducing the values for r_{CVC}, N and r_{CV} into Equation 4, we obtain a value of 960 MΩ for r_{RA}.

As previously mentioned, the CV potential is approximately 80 mV in the fluid-filling phase (Fig. 1A). An electric current needed to maintain 80 mV of potential across the CVC membrane of 60 MΩ resistance would be 1.3×10^{-9} A according to Ohm's law. If we assume the mean number of radial arms to be 10 for each CVC, the current generated by a single arm would be 1.3×10^{-10} A. This current would correspond to the transport of 8.3×10^{8} $H^+ s^{-1}$ across the membrane of a single radial arm by its V-ATPases. This value is obtained by dividing 1.3×10^{-10} C s^{-1} by e, the elementary electric charge (1.6×10^{-19} C). A current of 1.3×10^{-10} A across a membrane with a potential difference 80 mV is equivalent to 1.1×10^{-11} W. These values could be useful for an eventual understanding of the molecular mechanism of ion transport across the CVC membrane.

CV membrane potential during the rounding and fluid-discharging phases of the CVC cycle

The small potential (approximately 10 mV) seen during the rounding phase **(**R in Fig. 1A**)**, corresponds to an unexplained potential across the CV membrane itself. We recently found that the K^+ and Cl^- activities in the CV fluid are always approximately 2.5 times those in the cytosol (Stock et al., 2002). It is therefore possible that this 10 mV CV membrane potential corresponds to a potential value between two equilibrium potentials, one for K^+ (approximately –23 mV) and the other for Cl^- (approximately 23 mV). Studies on the putative ion channels in the CV membrane are needed to explain how an electrical potential is developed during the rounding phase. However, as pointed out by Tominaga et al. (1998), the potential measured during the fluid-discharging phase, 26 mV, corresponds to the plasma membrane potential since the CV pore is open during this phase and, therefore, the CV fluid is electrically connected to the external fluid.

This work was supported by NSF grant MCB 98 09929. We are grateful to Takashi Tominaga for his advice on electrical measurements and the computer control of the experiments. Our thanks go to the late Dr Ikuo Yasumasu for his suggestion that we use furosemide in our experiments. We particularly wish to thank Olav Sverre Berge for his help in developing the programs for capturing and processing the data. We also acknowledge the Norwegian Research Society (NFR) for financial support for H.K.G.

References

Allen, R. D. and Fok, A. K. (1988). Membrane dynamics of the contractile vacuole of *Paramecium*. *J. Protozool.* **35**, 63-71.

Allen, R. D. and Naitoh, Y. (2002). Osmoregulation and contractile vacuoles of protozoa. *Int. Rev. Cytol.* **215**, 351-394.

Allen, R. D., Ueno, M. S., Pollard, L. W. and Fok, A. K. (1990). Monoclonal antibody study of the decorated spongiome of the contractile vacuole complex of *Paramecium*. *J. Cell Sci.* **96**, 469-475.

Brater, D. C. (1998). Diuretic therapy. *N. Engl. J. Med.* **339**, 387-395.

Canessa, M., Brugnara, C., Cusi, D. and Tosteson, D. C. (1986). Modes of operation and variable stoichiometry of the furosemide-sensitive Na and K fluxes in human red cells. *J. Gen. Physiol.* **87**, 133-142.

Deitmer, J. W. and Schlue, W. R. (1989). An inwardly directed, electrogenic sodium bicarbonate co-transport in glial cells of the leech central nervous system. *J. Physiol., Lond.* **411**, 179-194.

Fok, A. K., Aihara, M. S., Ishida, M., Nolta, K. V., Steck, T. L. and Allen, R. D. (1995). The pegs on the decorated tubules of the contractile vacuole complex of *Paramecium* are proton pumps. *J. Cell Sci.* **108**, 3163-3170.

Fok, A. K. and Allen, R. D. (1979). Axenic *Paramecium caudatum*. I. Mass culture and structure. *J. Protozool.* **26**, 463-470.

Garay, R. C., Nazaret, C., Hannaert, P. A. and Cragoe, E. J., Jr (1988). Demonstration of a [K^+,Cl^-]-cotransport system in human red cells by its sensitivity to [(dihydroindeny)oxy]alkanoic acid: regulation of cell swelling and distinction from bumetanide-sensitive [Na^+,K^+,Cl^-]-cotransport system. *Mol. Pharmacol.* **33**, 696-701.

Hausmann, K. and Allen, R. D. (1977). Membranes and microtubules of the excretory apparatus of *Paramecium caudatum*. *Eur. J. Cell Biol.* **15**, 303-320.

Herrington, J., Newton, K. R. and Bookman, R. J. (1995). *Pulse Control V. 4.6: Igor Xops for Patch Clamp Data Acquisition and Capacitance Measurements*. Miami, FL: University of Miami.

Ishida, M., Aihara, M. S., Allen, R. D. and Fok, A. K. (1993). Osmoregulation in *Paramecium*: the locus of fluid segregation in the contractile vacuole complex. *J. Cell Sci.* **106**, 693-702.

Ishida, M., Fok, A. K., Aihara, M. S. and Allen, R. D. (1996). Hyperosmotic stress leads to reversible dissociation of the proton pump-bearing tubules from the contractile vacuole complex in *Paramecium*. *J. Cell Sci.* **109**, 229-237.

Lauf, P. K. (1984). Thiol-dependent passive K/Cl transport in sheep red cells. IV. Furosemide inhibition as a function of external Rb^+, Na^+, and Cl^-. *J. Membr. Biol.* **77**, 57-62.

Stock, C., Allen, R. D. and Naitoh, Y. (2001). How external osmolarity

affects the activity of the contractile vacuole complex, the cytosolic osmolarity and the water permeability of the plasma membrane in *Paramecium multimicronucleatum*. *J. Exp. Biol.* **204**, 291-304.

Stock, C., Grønlien, H. K., Allen, R. D. and Naitoh, Y. (2002). Osmoregulation in *Paramecium*: in situ ion gradients permit water to cascade through the cytosol to the contractile vacuole. *J. Cell Sci*. **115**, 2339-2348.

Tominaga, T., Allen, R. D. and Naitoh, Y. (1998). Electrophysiology of the *in situ* contractile vacuole complex of *Paramecium* reveals its membrane dynamics and electrogenic site during osmoregulatory activity. *J. Exp. Biol.* **201**, 451-460.

Woo, J.-T., Shinohara, C., Sakai, K., Hasumi, K. and Endo, A. (1992). Inhibition of the acidification of endosomes by antibiotic concanamycin B in macrophage J774. *Eur. J. Biochem*. **207**, 383-389.